Electrochemical textile dye removal using steel wool as an extended electrode

Gholamreza Mohamadian [1], Abbas Rezaee [1*], Hoshyar Hossini [1,2]

1 Environmental Health Department, Faculty of Medical Sciences, Tarbiat Modares University, Tehran, Iran
2 Department of Environmental Health Engineering, Faculty of Health, Kermanshah University of MedicalSciences, Kermanshah, Iran

Journal of Advanced Environmental Research and Technology

Vol. 1, No.3
page 35-44 ,summer 2023
***
Received 11 November 2023
Accepted 07 January 2024

Abstract

The current study suggests the utilization of steel wool as an extended anode electrode in an electrochemical process to enhance the efficiency of Remazol Brilliant Blue R (RBBR) removal from wastewater. The effect of the operating parameters of initial pH, applied current, supporting electrolyte, and initial dye concentration on textile dye removal efficiency was investigated to determine the optimum conditions of the process. Kinetic studies were performed in the optimum conditions. Scanning electron microscopy (SEM) and x-ray fluorescence (XRF) were carried out to determine the morphology and characterization of the extended anode surface. Under the optimum conditions, the dye and chemical oxygen demand (COD) removal were obtained 99.42% and 72.72%, respectively. The reaction kinetic data of the electrochemical process was followed by the pseudo-second-order kinetic rate equation ($R^2 = 0.99$). These findings might be useful in treating the various pollutants in industrial wastewater.

key words

Steel Wool

Electrochemical

Extended anode

Remazol Brilliant Blue R

Textile

*To whom correspondence should be addressed:
rezaee@modares.ac.ir

[DOI: 10.22034/jaert.1.3.35]

1. Introduction

Wastewater from textile factories contains organic and inorganic materials, auxiliary materials, and dyes that are characterized by chemical oxygen demand (COD) and color [1]. The discharge of this wastewater into the environment can have adverse effects that include oxygen deficiency in water sources, decreased light penetration into water sources, and photosynthesis [2, 3]. It has been estimated that approximately 15% of the dyes used in textile manufacturing end up in wastewater [4]. Textile dyes are typically categorized based on their chromophore groups, with azo dyes being a primary group used on an industrial scale. Remazol Brilliant Blue R (RBBR) is a popular azo dye employed as a precursor for the synthesis of polymeric dyes. As a polycyclic aromatic compound, RBBR is both toxic and resistant to degradation, posing a challenge as an organo-pollutant. Various methods have been proposed for treating color-contaminated textile wastewater, including adsorption, electrocoagulation, photocatalytic decolorization, and biological processes [1-7]. Electrochemical processes have been used as high-performance techniques that produce good-quality effluent. They have been successfully used for the treatment of wastewater produced by electroplating, laundries, latex particles, restaurants, and slaughterhouses [8, 9]. The process offers advantages such as low chemical requirements, low sludge production, compactness, and ease of operation. An electrochemical process involves the application of a direct current to an anode material, which undergoes oxidation, and a cathode that undergoes reduction. In the context of textile dye removal, electro-oxidation, adsorption, and coprecipitation have been employed to eliminate textile dyes from a solution matrix. The material and configuration of the electrode are important parameters for oxidation and coagulants for electrocoagulation. Fe, Al, and stainless steel anode electrodes are generally used for electrocoagulation. Stainless steel generates a low amount of sludge and shows high efficiency. Generally, limitation in the electrode surface area is a problem in the electrocoagulation process. Extended the surface of anode electrodes can address this problem [10, 11]. The present study proposes utilizing steel wool as an anode electrode. Steel wool is advantageous in this context due to its increased surface area and low susceptibility to corrosion. Comprising fine and soft steel filaments bundled in a fiber package, steel wool finds applications in various tasks such as finishing and repairing, polishing metal or wood materials, cleaning windows, household cookware, generating sparks, and sanding surfaces. This study proposes an extended anode electrode with increased surface area to provide better removal efficiency of the dye from wastewater. The steel wool will offer increased oxidation surfaces on all sides of the anode electrode.

2. Materials and Methods

2.1. Material

The RBBR was purchased from Dye Star (Germany). The characteristics and chemical structure of the dye are shown in Table 1.

An aqueous stock solution (1000 mg/l) of RBBR was prepared using deionized distilled water. Different concentrations of the dye were obtained by diluting the stock solution. All chemicals used in this study were of analytical reagent grade and

Table 1. The characterization of the RBBR dye

Chemical formula	$C_{22}H_{16}O_{11}N_2S_3Na_2$
Commercial name	Remazol Brilliant Blue
Class	Azo
Molecular weight (g/mol)	626.5
λmax	592
Molecular structure	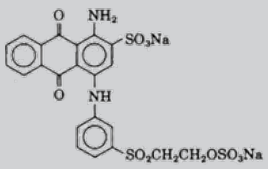

[DOI: 10.22034/jaert.1.3.35]

were used as received without further purification. The pH values were adjusted with H_2SO_4 in the acid range and NaOH in the alkaline range.

2.2. Experimental setup and operation

The reactor was constructed from a glass cylindrical chamber (18×10×6 cm) with a working volume of 800 ml. The steel wool and a stainless-steel plate (15×5×2 mm) were used as the extended cathode and anode, respectively. The cathode was placed in the center of the cylindrical reactor and the extended anode was placed around the cathode. The distance between the cathode and the anode was about 2 cm, which is a common distance for electrocoagulation. The pretreatment of the electrode was carried out by immersing it in 0.1M H_2SO_4 and then washing it with deionized water. The electrical current was induced to the electrodes by a DC power supply (Atten ASP3005S-3D, China) with a galvanostatic option for controlling the current and voltage. The NaCl as the supporting electrolyte was provided to the solution for increasing the conductivity. The effect of the operating parameters of applied current (100-1000 mA/cm^2), pH (6 to 9), and reactive time (0-15 min) for the use of the extended anode was evaluated for decolorization efficiency. Experiments were carried out under normal laboratory conditions and room temperatures. Each experiment was repeated at least three times.

2.3. Analysis

Samples were withdrawn from the reactor at specific time intervals to measure the COD and the absorption spectra at a wavelength of 592 nm using a spectrophotometer (UV Ray, China). The samples were filtered through a 0.45 µm porosity polytetrafluoroethylene filter before chemical analysis. The pH values were determined using a portable pH-tester (Oaklon, Malaysia). The morphological features of the anode electrode and sludge samples were evaluated using a light microscope (Siemens, Germany) and by SEM (Philips, X'Pert MPD; tube: Cu k α, λ: 1.54056 A°, step size: 0.02°/s, voltage: 40 kV, current: 30 mA). The XRF pattern was recorded on a Philips PW2404 spectrometer that used Cu Kα radiation. The concentration of the RBBR in the treated solution was determined spectrophotometrically. The decolorization efficiency was calculated (Eq. 1):

$$decolorization\ efficiency\ (\%) = \frac{C_0 - C_f}{C_0} \times 100 \qquad (1)$$

where C_0 and Cf are the initial concentration and the concentration at any time t of the dye. The COD of the RBBR solutions was measured using standard methods for the examination of water and wastewater [12].

3. Results and Discussion

3.1. Effect of applied current

The applied current influences the efficiency of decolorization during electrocoagulation. Controlling the amount of applied current is a method of regulating the reaction rate [13]. The effect of

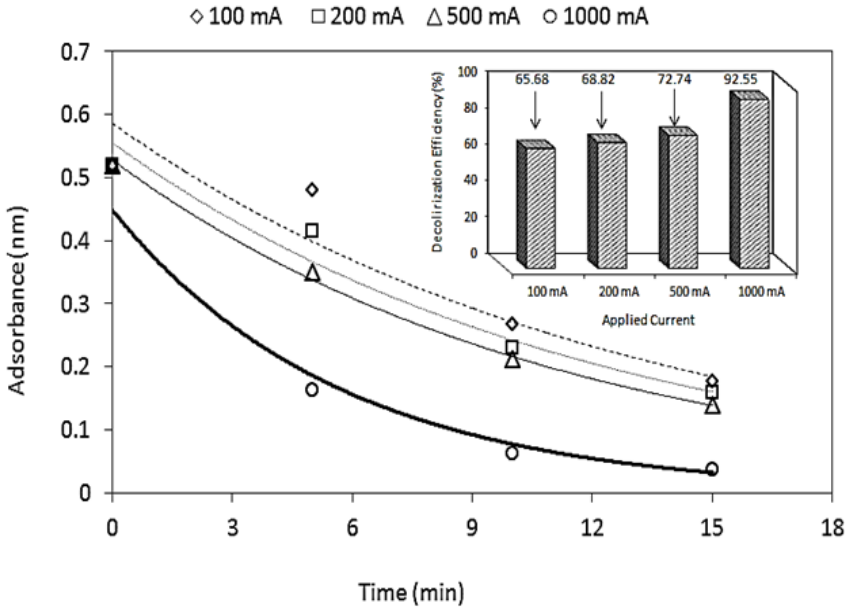

Fig. 1. Effect of applied current on dye adsorption spectrum and dye removal efficiency (electrocoagulation conditions: C0: 300 mg/L, time: 15 min, NaCl= 0.3 g/L).

[DOI: 10.22034/jaert.1.3.35]

applied current was evaluated on the decolorization efficiency at various applied currents (100-1000 mA). The results show that increasing the applied current increased decolorization (Fig. 1).

The color removal percentages were obtained at 65.68%, 68.82%, 72.74%, and 92.55% using 100, 200, 500, and 1000 mA induced current, respectively. It was found that the rate of color removal is proportional to the dye concentration in the solution when accounting for Faradaic currents. The rate of release of iron ions into the solution from the iron anode followed Faraday's law [14]. It was observed that higher currents generated a significant amount of iron ions, which in turn trapped the dye molecules and increased removal efficiency.

3.2. Effect of initial pH

The influence of pH on the efficiency of electrocoagulation has been documented [15]. In the investigation of dye removal through electrocoagulation with stainless steel electrodes, the impact of pH on the process was explored. Dye solutions were adjusted to pH values ranging from 3 to 9 by the addition of H_2SO_4 or NaOH as necessary. The findings demonstrated that the highest color removal efficiency was achieved at pH 3. It can be inferred that acidic pH enhances removal efficiency when utilizing stainless steel electrodes. At low pH, ferrous ions undergo conversion to ferric ions. In such conditions, the formed coagulants persist in the aqueous solution, effectively removing pollutants through adsorption or coprecipitation mechanisms. The rate of this conversion is greatly affected by the pH and surface charge of the coagulating particle. Different pH values produce different forms of Fe species, including monomeric ions, ferric hydroxyl complexes with hydroxide ions, and polymeric forms such as $Fe(H_2O)_6^{3+}$, $Fe(H_2O)_5OH^{2+}$, $Fe(H_2O)_4(OH)^{2+}$, $Fe_2(H_2O)_8(OH)_2^{4+}$, $Fe_2(H_2O)_6(OH)_4^{2+}$ and $Fe(OH)^{4-}$ [16]. The main mechanisms for electrocoagulation and generation of metal hydroxides are shown in Table 2.

3.3. Effect of supporting electrolyte concentration

Fig. 2 shows the effect of NaCl as a supporting electrolyte on dye removal.

The findings indicate that the addition of 0.5 g/l NaCl led to higher color removal. This implies

Table 2. The mechanisms of the metal hydroxides generating under various pH values

pH < 4	4 < pH < 7	6 < pH < 9
Anode $4Fe_{(s)} \rightarrow 4Fe_{(aq)}^{2+} + 8e^-$ Bulk of solution : $4Fe_{(aq)}^{2+} + 10H_2O_{(l)} + O_{2(aq)} \rightarrow 4Fe(OH)_{3(s)} + 8H^+_{(aq)}$ Cathode: $8H^+_{(aq)} + 8e^- \rightarrow 4H_{2(g)}$ Overall: $4Fe_{(s)} + 10H_2O_{(l)} + O_{2(aq)} \rightarrow 4Fe(OH)_{3(s)} + 4H_{2(g)}$	Anode: $4Fe_{(s)} + 24H_2O_{(l)} \rightarrow 4Fe(H_2O)_4(OH)_{2(aq)} + 8H^+ + 8e^-$ Bulk of solution: $4Fe(H_2O)_4(OH)_{2(aq)} + O_{2(aq)} \rightarrow 4Fe(H_2O)_3(OH)_{3(s)} + 2H_2O_{(l)}$ Bulk of solution: $4Fe(H_2O)_3(OH)_{3(s)} \rightarrow 2Fe_2O_3(H_2O)_{6(s)} + 6H_2O_{(l)}$ Cathode: $8H^+_{(aq)} + 8e^- \rightarrow 4H_{2(g)}$	Bulk of solution: $4Fe(H_2O)_4(OH)_{2(aq)} \rightarrow 4Fe(H_2O)_4(OH)_{2(s)}$

pH < 4	4 < pH < 9
Anode: $Fe_{(s)} \rightarrow Fe^{2+}_{(aq)} + 2e^-$ Cathode: $2H^+ + 2e^- \rightarrow H_{2(g)}$ Overall: $Fe_{(s)} + 2H^+ \rightarrow Fe^{2+}_{(aq)} + H_{2(g)}$	Anode: $Fe_{(s)} + 6H_2O_{(l)} \rightarrow Fe(H_2O)_4(OH)_{2(aq)} + 2H^+ + 2e^-$ Cathode: $2H^+ + 2e^- \rightarrow H_{2(g)}$ Overall: $Fe_{(s)} + 6H_2O_{(l)} \rightarrow Fe(H_2O)_4(OH)_{2(s)} + H_{2(g)}$ Bulk of solution: $Fe(H_2O)_4(OH)_{2(aq)} \rightarrow Fe(H_2O)_4(OH)_{2(s)}$

4 < pH < 9
Anode: $2Fe_{(s)} + 12H_2O_{(l)} \rightarrow 2Fe(H_2O)_3(OH)_{3(aq)} + 6H^+ + 6e^-$ Bulk of solution: $2Fe(H_2O)_3(OH)_{3(aq)} \rightarrow 2Fe(H_2O)_3(OH)_{3(s)}$ Bulk of solution: $2Fe(H_2O)_3(OH)_{3(s)} \rightarrow Fe_2O_3(H_2O)_{6(s)} + 3H_2O_{(l)}$ Cathode: $6H^+ + 6e^- \rightarrow 3H_{2(g)}$ Overall: $2Fe_{(s)} + 9H_2O_{(l)} \rightarrow Fe_2O_3(H_2O)_{6(s)} + 3H_{2(g)}$

[DOI: 10.22034/jaert.1.3.35]

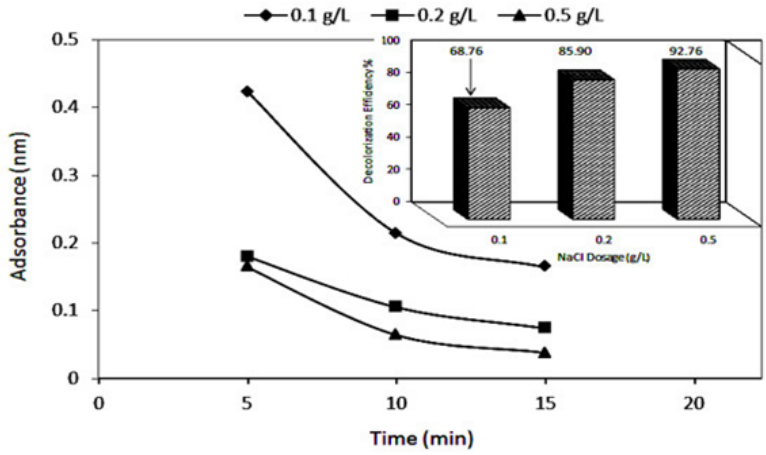

Fig. 2. Effect of NaCl concentration on dye adsorption spectrum and dye removal efficiency (electrocoagulation conditions: C0: 300 mg/L, time: 15 min, applied current: 200 mA).

that the presence of a supporting electrolyte enhanced the efficiency of RBBR dye removal. As the concentration of the supporting electrolyte increased from 0.1 to 0.5 g/l, there was a substantial improvement in removal efficiency, rising from 68.76% to 92.76%. However, concentrations of NaCl above 0.5 g/l did not yield a significant enhancement in dye removal efficiency. Consequently, a value of 0.5 g/l NaCl was chosen as the optimum concentration for the color removal experiments. The conductivity of the solution affects electrocoagulation. Solution conductivity affects the current efficiency, voltage, and energy savings during electrocoagulation because the current passing through the electrolyte is a function of the conductivity of the different voltages. One method used to overcome this problem is to add electrolytes to increase the electrical conductivity of the solution and decrease energy consumption. Generally, the conductivity of the solution increases as the supporting electrolyte concentration increases [16]. NaCl was used as the supporting electrolyte to increase the conductivity of the aqueous solution. NaCl is broken down to produce the highly oxidative reagents of chlorine, hypochlorous acid, hypochlorite, and hypochlorite ions from the chloride ions at the anode surface [17]. It has been reported that using NaCl as a supporting electrolyte allows chloride ions to significantly decrease the adverse effects of other anions, such as HCO^{3-} and SO_4^{2-}. The carbonate ion precipitates the calcium ions that form an insulating layer on the surface of the cathode which increases the ohmic resistance of the electrochemical cell [18].

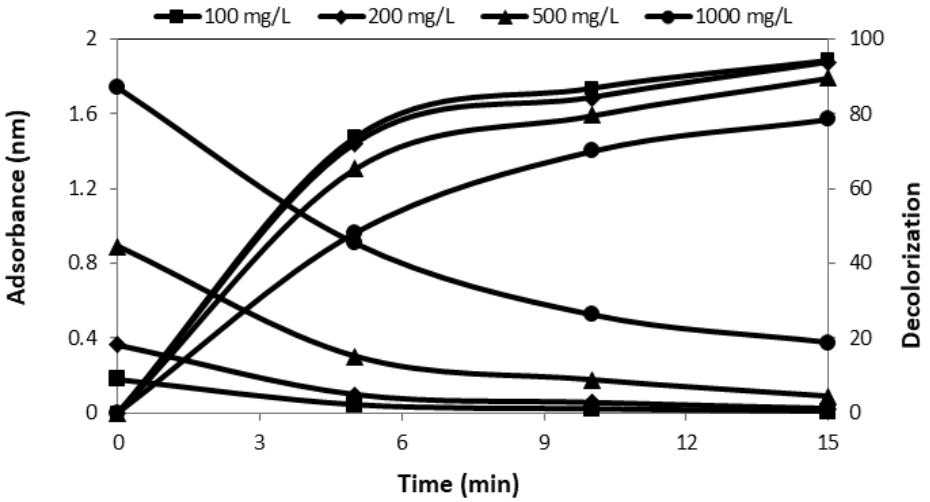

Fig. 3. Effect of initial dye concentrations on dye adsorption spectrum and dye removal efficiency (electrocoagulation conditions: C0: 300 mg/L; time: 15 min; applied current: 200 mA; NaCl: 0.5 g/L).

[DOI: 10.22034/jaert.1.3.35]

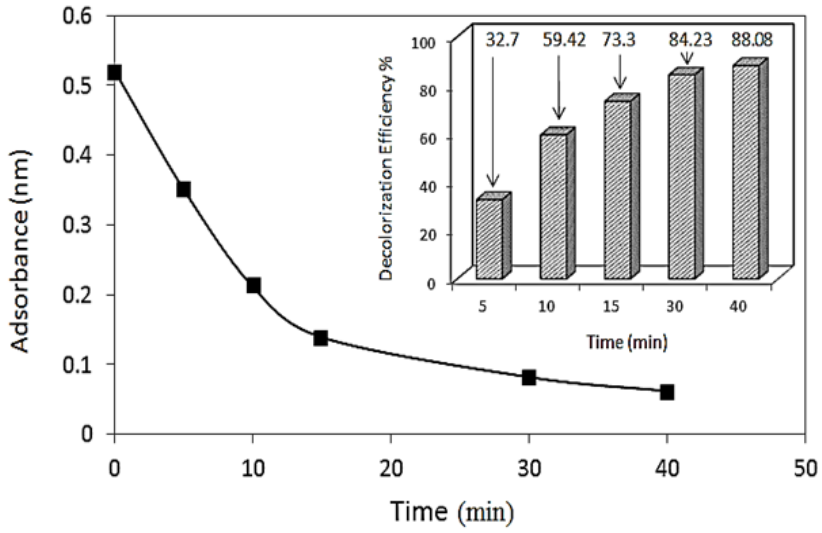

Fig. 4. Effect of reaction time on dye adsorption spectrum and removal efficiency (electrocoagulation conditions: applied current: 200 mA, NaCl: 0.5 g/L).

3.4. Effect of initial concentration of RBBR dye

RBBR solution at initial concentrations of 100–1000 mg/l was treated by electrocoagulation under optimized conditions. Fig. 3 shows the initial dye concentration versus RBBR removal efficiency.

The results revealed that an increase in initial dye concentration decreased decolorization efficiency, probably in accordance with Faraday's law. At high RBBR concentrations, the flocs produced were insufficient to adsorb all dye molecules in the solution [19].

3.5. Effect of reaction time

The reaction time determines the production rate of coagulants and oxidant agents from the anode electrodes. Fig. 4 shows the relationship between dye removal efficiency and reaction times of 5 to 40 min.

The results indicate that significant dye removal was obtained within 15 min (~73.3%). As seen, dye removal increased rapidly for 15 min, the rate of increase then slowed and did not improve much beyond 40 min of treatment. The role of reactive time can be explained by Faraday's law (Eq. 2):

$$A_m = I \cdot t \cdot m / n c \qquad \text{Eq. 2}$$

where Am is the amount of dissolved anode material (g); I is the current intensity (A); t is the run time (s); m is the specific molecular weight (g/mol); n is the number of electrons involved; and c is Faraday's constant (As/mol).

3.6. COD removal

The COD and dye removal efficiencies were analyzed under optimal experimental conditions.

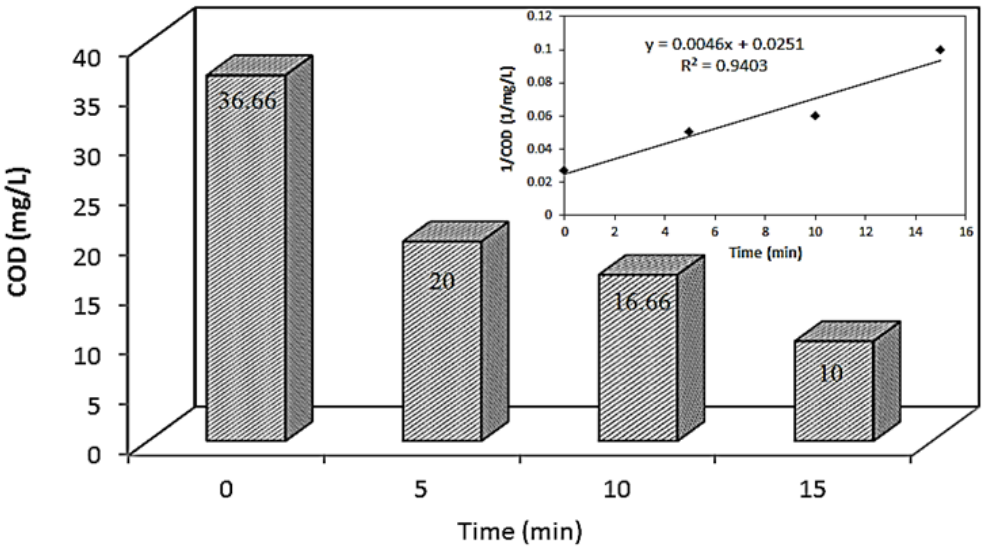

Fig. 5. The trend of COD removal during the electrocoagulation process and kinetic of COD removal.

[DOI: 10.22034/jaert.1.3.35]

Table 3. Kinetic constants and related parameters

Kinetic model	**Pseudo-first order**			
Conc. mg/L	100	200	500	1000
Linear Eq.	y =-0.1192x + 4.4907	y = 0.1495x + 5.0936	y = 0.1473x + 6.0968	y = 0.1032x + 6.8325
R^2	0.9633	0.9322	0.9473	0.9405
K_1 (min-1)	0.1192	0.1495	0.1473	0.1032
Simpled Eq.	$C_t = 100 \times e^{-0.1192.t}$	$C_t = 200 \times e^{-0.1495.t}$	$C_t = 500 \times e^{-0.1473.t}$	$C_t = 1000 \times e^{-0.1032.t}$
Kinetic model	**Pseudo-second order**			
Conc. mg/L	100	200	500	1000
Linear Eq.	y = 0.0034x + 0.0082	y = 0.0029x + 0.0038	y = 0.0011x + 0.0008	y = 0.0002x + 0.0009
R^2	0.9921	0.9908	0.9832	0.9929
K_2 (L/g. min)	0.0034	0.0029	0.0011	0.0002
Simpled Eq.	$\frac{1}{C_t} = 0.0034.t + 0.01$	$\frac{1}{C_t} = 0.0018.t + 0.005$	$\frac{1}{C_t} = 0.0011.t + 0.002$	$\frac{1}{C_t} = 0.0002.t + 0.001$

The maximum efficiency for COD removal was 99.42%. The kinetic constant for COD removal was 0.0046 and the higher correlation coefficient (R^2) was ~0.94 (Fig. 5).

3.7. Kinetic studies

First- and second-order kinetic models were evaluated. The equations were expressed as [20]:

$$\ln C_t = \ln C_0 - k_1 t \quad \text{(-Ln Ct v.s time)} \qquad \text{(Eq.3)}$$

where C0 is the initial dye concentration; Ct is the terminal dye concentration (t); k_1 and k_2 are the first- and second-order kinetic constants, respectively. The slopes and the linear equations of the kinetic plots (data not shown), constants, correlation coefficients, and interpretations were determined. The kinetic parameters as calculated in Eqs. (10) and (11) are presented in Table 3.

As seen, the pseudo-second-order kinetic model provided a better R^2 value, indicating that it better describes the kinetics. The number of oxidative species required and coagulant produced electrochemically for dye removal increased as the dye concentration increased, which decreased the removal and diffusion rates [21].

3.8. Morphology and structure analysis

The sludge's morphological features and chemical analysis were evaluated using SEM and XRF.

The sludge was collected from the reactor at the optimal time and the samples were filtered through a Whatman #41 filter paper before analysis. The SEM results are shown in Fig. 6 and the XRF results are shown in Table. 4. The electrode surface was observed to be dark with corrosion. The for-

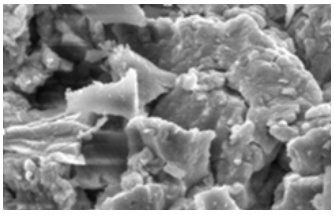

Fig. 6. SEM micrograph of sludge particles after electrocoagulation (Magnification, X5000).

[DOI: 10.22034/jaert.1.3.35]

Table 4. XRF analysis of electrocoagulation sludge

Constituents	L.O.I.	Na_2O	MgO	SiO_2	SO_3	Cl	Fe_2O_3	Cr
(%)	32.256	1.977	0.345	0.957	5.195	2.865	45.641	5.016

mation of dark areas can be attributed to the consumption of anode material at active sites from the generation of coagulants and oxidative agents. The presence of Fe_2O_3, Na_2O, Cl, Cr, MgO, SiO_2, and SO_3 in the sludge was confirmed by XRF of the sample (Table 4).

The RBBR was destabilized and separated from the wastewater by the Fe_2O_3 generated during electrocoagulation. The microscopic images reflect the relative sizes of the coagulant and the aggregated formation.

4. Conclusions

The proposed steel wool as an extended anode was shown to be an effective electrode for RBBR dye removal. The following conclusions were drawn from this study:

• A maximum dye removal efficiency of 99.42% was achieved using steel wool as an extended anode.

• The pH value of 4.0 presented higher dye removal

• The kinetic data showed that RBBR dye removal during the electrochemical process can be described using a second-order kinetic model.

• The kinetic constant for COD removal was obtained at ~0.0046.

• The COD decreased by more than 72% in dye solutions containing RBBR.

• XRF analysis confirms that a large portion of sludge consisted of iron oxide (Fe_2O_3).

Acknowledgments

The authors would like to thank the Tarbiat Modares university for the support provided.

[DOI: 10.22034/jaert.1.3.35]

References

[1] R.M.F. Beuto, M.R. Almeida, P. Bharmoria, M. Freire, A.P.M., Tavares, Improvements in the enzymatic degradation of textile dyes using ionic-liquid-based surfactants, Sep. Purif. Technol. 235 (2020), 116191, https://doi.org/10.1016/j.seppur.2019.116191

[2] Wang, Y.; Wang, H.; Wang, X.; Xiao, Y.; Zhou, Y.; Sun, X.; Cai, J.; Sun, F., Resuscitation, isolation and immobilization of bacterial species for efficient textile wastewater treatment: A critical review and update, Sci Total Environ. 2020, 730, 139034, https://doi.org/10.1016/j.scitotenv.2020.139034

[3] Patil, C.S.; Kadam, A.N.; Gunjal, D.B.; Naik, V.M.; Lee, S-W.; Kolekar, G.B.; Gore, A.S., Sugarcane molasses derived carbon sheet@sea sand composite for direct removal of methylene blue from textile wastewater: Industrial wastewater remediation through sustainable, greener, and scalable methodology, Sep Purif Technol 2020, 247, 116997, https://doi.org/10.1016/j.seppur.2020.116997

[4] Al-Amrani, W.A.; Lim, P.E.; Seng, C.-E.; Ngah, W.S.W., Factors affecting bio-decolorization of azo dyes and COD removal in anoxic–aerobic react operated sequencing batch reactor. J Taiwan Inst Chem Eng 2014, 45, 609-616. https://doi.org/10.1016/j.jtice.2013.06.032

[5] Syafiuddin, A.; Fulazzaky, M.A., Decolorization kinetics and mass transfer mechanisms of Remazol Brilliant Blue R dye mediated by different fungi, Biotechnol Report 2021, 29, 200573, https://doi.org/10.1016/j.btre.2020.e00573

[6] Kuleyin, A.A.; Gok, A.; Akbal, F., Treatment of textile industry wastewater by electro-Fenton process using graphite electrodes in batch and continuous mode, J Environ Chem Eng 2021, 104, 104782, https://doi.org/10.1016/j.jece.2020.104782

[7] Reghiaua, A.; Barkat, D.; Jawad, A.H.; Abdulhameed, A.S.; Rangabhashiam, S, Rezwan Khan, M.; Alothman, Z.A., Magnetic Chitosan-Glutaraldehyde/Zinc Oxide/Fe3O4 Nanocomposite: Optimization and Adsorptive Mechanism of Remazol Brilliant Blue R Dye Removal, J Polymer Environ 2021, e00573, https://doi.org/10.1016/j.btre.2020.e00573

[8] Hoseinzadeh, E.; Rezaee, A.; Fazeli, S., Electrochemical denitrification using carbon cloth as an efficient anode, Desalination Water Treat., 2017, 97, 244-250. 10.5004/dwt.201x.21692

[9] Nidheeesh, P.V.; Kumar, A.; Babu, D.S.; Scaria, J.; Kumar, M.S., Treatment of mixed industrial wastewater by electrocoagulation and indirect electrochemical oxidation, Chemosphere, 2020, 251, 126437, https://doi.org/10.1016/j.chemosphere.2020.126437

[10] Shao, D.; Zhang, X.; Wang, Z.; Zhang, Y.; Tan, G.; Yan, W., New architecture of a variable anode for full-time efficient electrochemical oxidation of organic wastewater with variable Cl− concentration, Appl Surf Sci 2020, 512, 146003, https://doi.org/10.1016/j.apsusc.2020.146003

[11] Loloi, M.; Rezaee, A.; Aliofkhazraei, M.; Sabour Rouhaghdam, A., Electrocatalytic oxidation of phenol from wastewater using Ti/SnO2–Sb_2O_4 electrode: chemical reaction pathway study, Environ Sci Pollut Res 2016, 23, 19735–19743. https://doi.org/10.1007/s11356-016-7110-6

[12] American Public Health Association (APHA) Standard Methods for the Examination of Water and Wastewater,17th ed. 1995 APHA, Washington, DC.

[13] Zhou, Y.; Zhang, Y.; Li, Z.; Hao, C.; Wang, Y.; Li, Y.; Dang, Y.; Sun, X.; Hau, G.; Fu, Y., Oxygen reduction reaction electrocatalysis inducing Fenton-like processes with enhanced electrocatalytic performance based on mesoporous ZnO/CuO cathodes: Treatment of organic wastewater and catalytic principle, Chemosphere, 2020, 259, 127463, https://doi.org/10.1016/j.chemosphere.2020.127463

[14] Wang, J.; Yao, J.; Wang, L.; Xue, Q.; Hu, Z.; Pan, B., Multivariate optimization of the pulse electrochemical oxidation for treating recalcitrant dye wastewater, Sep Purif Technol 2020, 230, 115851, https://doi.org/10.1016/j.seppur.2019.115851

[15] Aleboyeh, A.; Daneshvar, N.; Kasiri, M.B. , Optimization of C.I. Acid Red 14 azo dye removal by electrocoagulation batch process with response surface methodology, Chem Eng Process 2008, 47, 827-832. https://doi.org/10.1016/j.cep.2007.01.033

[DOI: 10.22034/jaert.1.3.35]

[16] Khan, S.; Khan, H.; Anwar, S.; Khan, S.; Zanoni, M.V.B.; Hussain, S. Computational and statistical modeling for parameters optimization of electrochemical decontamination of synozol red dye wastewater, Chemosphere, 2020, 253, 126673, https://doi.org/10.1016/j.chemosphere.2020.126673

[17] El-Ghenymy, A.; Alsheyab, M.; Khodary, A.; Sires, I.; Abdel-Waheb, A., Corrosion behavior of pure titanium anodes in saline medium and their performance for humic acid removal by electrocoagulation, Chemosphere, 2020, 246, 125674, https://doi.org/10.1016/j.chemosphere.2019.125674

[18] Szpyrkowicz, L.; Juzzolino, C.; Kaul, S.N.; Daniele, S.; Faveri, M.D.D. , Electrochemical oxidation of dyeing baths bearing disperse dyes, Ind Eng Chem Res 2000, 39, 3241-3248. https://doi.org/10.1021/ie9908480

[19] Chen, H.; Zhang, Y.J.; He, P.Y.; Li, C.Y.; Li, H.H., Coupling of self-supporting geopolymer membrane with intercepted Cr(III) for dye wastewater treatment by hybrid photocatalysis and membrane separation, Appli Surf Sci 2020, 515, 146024, https://doi.org/10.1016/j.apsusc.2020.146024

[20] Nandi, B.K.; Patel, S., Removal of brilliant green from aqueous solution by electrocoagulation using aluminum electrodes: experimental, kinetics, and modeling, Sep Sci Technol 2014, 49, 601-612. https://doi.org/10.1080/01496395.2013.838682

[21] Kim, T.H.; Park, C.; Shin, E.B. , Decolorization of disperse and reactive dyes by continuous electrocoagulation process, Desalination 2002, 150, 165-175. https://doi.org/10.1016/S0011-9164(02)00941-4

[DOI: 10.22034/jaert.1.3.35]